Available online at www.sciencedirect.com
ScienceDirect
Journal of Catalysis 247 (2007) 137–144
JOURNAL OF CATALYSIS
www.elsevier.com/locate/jcat

Selective catalytic reduction of NO_x by H_2 using proton conductors as catalyst supports

Atsuko Tomita [a], Takeshi Yoshii [b], Shinya Teranishi [b], Masahiro Nagao [b], Takashi Hibino [b,*]

[a] *Materials Research Institute for Sustainable Development, National Institute of Advanced Industrial Science and Technology, Moriyama-ku, Nagoya 463-8560, Japan*

[b] *Graduate School of Environmental Studies, Nagoya University, Nagoya 464-8601, Japan*

Received 13 November 2006; revised 25 January 2007; accepted 1 February 2007

Available online 2 March 2007

Abstract

The selective catalytic reduction (SCR) of NO_x by H_2 was studied using proton-conducting $Sn_{0.9}In_{0.1}P_2O_7$ as a catalyst support at 50–350 °C. When a mixture of 800 ppm NO, 1400–8400 ppm H_2, and 5% O_2 in Ar was introduced to the Pt/C working electrode, NO_x was reduced to N_2 with N_2 selectivity values >80%. The reaction mechanism was shown to be based on a mixed potential at the Pt/C working electrode. This mechanism was also applicable to a $Sn_{0.9}In_{0.1}P_2O_7$-supported Pt catalyst. H_2 SCR over the Pt/$Sn_{0.9}In_{0.1}P_2O_7$ catalyst was characterized by a wide operating temperature window (50–350 °C) and remarkable N_2 selectivity values (>80%). Catalyst performance could be further improved by the addition of Rh to Pt, in which NO_x conversion was a maximum 1.4 times higher than that over the Pt/$Sn_{0.9}In_{0.1}P_2O_7$ catalyst and N_2 selectivity was increased to >89% at all temperatures tested.

Keywords: Selective catalytic reduction; NO_x; Hydrogen; Proton conductor

1. Introduction

NO_x (NO and NO_2), produced by the combustion of fuels, are major air pollutants responsible for photochemical smog, acid rain, ozone depletion, and the greenhouse effect. Vehicular and stationary combustion processes contribute up to 90% or more of the global NO_x production [1]. Consequently, a number of de-NO_x techniques have been investigated, especially for diesel and lean-burning gasoline engines that emit exhaust with excess O_2, for which the commonly used three-way catalyst is not effective for the reduction of NO_x to N_2. Selective catalytic reduction (SCR) of NO_x using NH_3 [2,3], urea [4,5], and hydrocarbons [6–8] as reducing agents is widely viewed as a promising de-NO_x technology. However, NH_3 and urea require storage tanks and frequent replenishment. Moreover, hydrocarbons need to be operated at temperatures above 200 °C because of their low reactivity.

In recent years, the use of H_2 as an alternate reducing agent for NO_x has received significant attention because of its presence in automobile exhaust and its high reactivity at temperatures below 200 °C [9–15]. The following reactions occur in the $NO/H_2/O_2$ system:

$$2NO + 4H_2 + O_2 \rightarrow N_2 + 4H_2O \quad (1)$$

and

$$2NO + 3H_2 + O_2 \rightarrow N_2O + 3H_2O. \quad (2)$$

Various studies have reported that Pt-based support catalysts are active for the above reactions. NO is dissociated into $N_{(ad)}$ and $O_{(ad)}$ on Pt clusters, promoted by previously adsorbed $H_{(ad)}$ [9,10]. Burch and Coleman proposed that N_2 and N_2O are formed through the combination of $N_{(ad)}$ with each other and with another molecular NO, respectively [11]. NH_3 formation was also found to occur by the reaction of $N_{(ad)}$ with $H_{(ad)}$ at high temperatures [12]. Shibata et al. found that the reaction of NO with the NH_3 formed is another important reaction pathway for H_2 SCR [13].

* Corresponding author.
E-mail address: hibino@urban.env.nagoya-u.ac.jp (T. Hibino).

0021-9517/$ – see front matter
doi:10.1016/j.jcat.2007.02.001

The above reaction mechanism is strongly dependent on the catalyst support. Yokota et al. found that the activity order of the tested supports was ZSM-5 ∼ mordenite > SiO_2 > Al_2O_3 [14]. They also developed a Pt–Mo–Na/SiO_2 catalyst with a wider temperature window (especially for NO_x conversion) compared with the Pt/zeolite catalysts. Costa et al. investigated the use of $La_{0.5}Ce_{0.5}MnO_3$ as a potential support for Pt [15] and found that it improved the selectivity toward N_2 at 100–200 °C.

We recently investigated the feasibility and efficacy of using intermediate-temperature proton conductors as catalyst supports for H_2 SCR. $Sn_{0.9}In_{0.1}P_2O_7$ is a promising anhydrous proton conductor because of its high proton conductivity of $\geqslant 0.1$ S cm^{-1} under dehumidified conditions at 100–300 °C [16,17]. This material has a cubic structure, with Sn(or In)O_6 octahedra at the corners and P_2O_7 units at the edges. Protons migrate via the dissociation of hydrogen bonds with oxide ions in the P_2O_7 units by a hopping mechanism. We also applied this material as a solid electrolyte in various electrochemical devices. In a fuel cell, the H_2 oxidation shown in reaction (3) proceeded very easily over a Pt/C electrode [18]. On the other hand, in an electrolyzer, the NO reduction shown in reaction (4) was achieved with high current efficiencies over the same Pt/C electrode [19],

$$H_2 \rightarrow 2H^+ + 2e^- \tag{3}$$

and

$$NO + 2H^+ + 2e^- \rightarrow \frac{1}{2}N_2 + H_2O. \tag{4}$$

These reactions suggest that if $Sn_{0.9}In_{0.1}P_2O_7$ is used as a catalyst support, a new route to reduce NO_x to N_2 could be established for H_2 SCR. Namely, in the NO/H_2/O_2 system, a local galvanic cell is formed at the catalyst–support interface, as displayed in Scheme 1. As a result, the two reactions (3) and (4) proceed at the interface simultaneously due to self-discharge. This is similar to the corrosion behavior of metals in acid solutions, which in principle can be distinguished from conventional H_2 SCR.

The purpose of this study was to demonstrate the above concept by various electrochemical techniques and to develop a highly active and selective $Sn_{0.9}In_{0.1}P_2O_7$-supported catalyst for H_2 SCR. First, we fabricated an electrochemical cell consisting of an $Sn_{0.9}In_{0.1}P_2O_7$ electrolyte and a Pt/C working electrode, to measure the activity and potential of the working electrode under open-circuit conditions. We then prepared a Pt/$Sn_{0.9}In_{0.1}P_2O_7$ catalyst and evaluated its activity and selectivity toward N_2 in the temperature range of 50–350 °C. Finally, we attempted to improve the performance of the Pt/$Sn_{0.9}In_{0.1}P_2O_7$ catalyst by adding Rh to Pt.

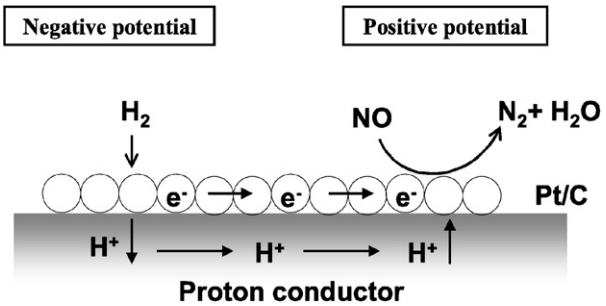

Scheme 1.

2. Experimental

2.1. Electrochemical cell studies

Fig. 1 shows an electrochemical cell used for measuring the activity and potential of a Pt/C working electrode. $Sn_{1-x}In_xP_2O_7$ ($x = 0$–0.1) samples were prepared in the same manner as reported previously [16–19]. The corresponding oxides (SnO_2 and In_2O_3) were mixed with 85% H_3PO_4 and ion-exchanged water and held under stirring at 300 °C until a high-viscosity paste was formed. This paste was calcined in an alumina pot at 650 °C for 2.5 h and then ground in a mortar with a pestle. The composition of $Sn_{1-x}In_xP_2O_7$ was determined by X-ray fluorescence (XRF) analysis. X-ray diffraction (XRD) analysis showed that $Sn_{1-x}In_xP_2O_7$ had a cubic single phase in the tested range of x of 0–0.1. Finally, the compound powders were pressed into pellets (12 mm i.d., about 1.5 mm thick) under 100 MPa pressure. Unless stated otherwise, all electrochemical measurements were conducted using $Sn_{0.9}In_{0.1}P_2O_7$ as the solid electrolyte. For comparison, silica and yttria-stabilized zirconia (YSZ) pellets were also used as solid electrolytes in the electrochemical cell. The working electrode (area, 0.5 cm^2) consisted of 10 wt% Pt/C or 10 wt% PtM, (M = Rh, Ir, Ru, Pd, Co) catalyst (E-TEK) and carbon paper (Toray, TGPH-090), wherein the atomic ratio of Pt to M was 4. The counterelectrode was the same Pt/C electrode as above.

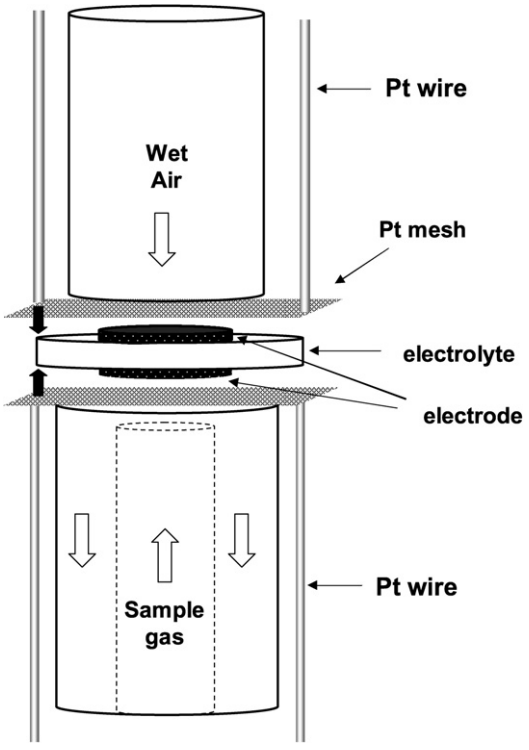

Fig. 1. Schematic illustration of the electrochemical cell.

A Pt reference electrode was attached to the side face of the electrolyte pellet.

The working electrode was supplied with a mixture of 800 ppm NO, 1400–8400 ppm H_2, 2–9% O_2, 0–4% H_2O vapor, and 0–10% CO_2 in Ar at a flow rate of 50 mL min^{-1}. The counter and reference electrodes were exposed to atmospheric air. The concentrations of NO_x and N_2 in the outlet gas from the working electrode were monitored using an online NO_x gas analyzer (Horiba, PG-225) and gas chromatograph (Shimazu, GC-8A), respectively. The gas concentrations were obtained after the reaction steady state was attained. The difference in potential (i.e., open-circuit voltage [OCV]) between the working and counter electrodes was measured with a digital electrometer (Hokuto Denko HE-104). Polarization and impedance measurements were made by controlling the potential of the working electrode versus that of the reference electrode with a potentiostat (Hokuto Denko HA-501) and impedance analyzer (Solartron SI-1260), respectively.

2.2. Catalyst studies

$Pt/Sn_{0.9}In_{0.1}P_2O_7$ (Pt content = 0.2–0.8 wt%) and $PtRh/Sn_{0.9}In_{0.1}P_2O_7$ (PtRh content = 0.8 wt%; Pt/Rh atomic ratio = 4) catalysts were prepared by impregnating $Sn_{0.9}In_{0.1}P_2O_7$ powders with aqueous solutions of the corresponding nitrates. After impregnation, the catalysts were dried in air at 110 °C for 12 h and then heated in Ar at 200 °C for 1 h. N_2 physisorption measurements (Bel Japan BELSORP-28SP) found a BET surface area of the catalyst support of $\leqslant 0.5$ $m^2\,g^{-1}$. Catalytic measurements were carried out in a fixed-bed flow reactor. A mixture of 800 ppm NO, 8400 ppm H_2, and 5% O_2 in Ar was passed through the catalyst (weight, 0.1 g) at a flow rate of 50 mL min^{-1}. The analysis of the outlet gas was carried out as described above.

3. Results and discussion

3.1. Electrochemical cell studies

Table 1 shows OCVs generated from the electrochemical cell by feeding various gas mixtures (0–1600 ppm pf NO, 0–8400 ppm H_2, 5% O_2, and 0.6% H_2O vapor in Ar) into the Pt/C working electrode at 250 °C. In the absence of H_2 and NO, the electrochemical cell yielded an OCV of +20 mV. This OCV value is more positive than the value (−16 mV) calculated from Nernst's equation (5) for an oxygen concentration cell and is in good agreement with the value (+20 mV) calculated from Nernst's equation (6) for a steam concentration cell [20]:

$$E = -(RT/4F)\ln[P_{O_2(\text{counter})}/P_{O_2(\text{working})}], \quad (5)$$

$$E = -(RT/2F)\ln[P_{H_2O(\text{working})}/P_{H_2O(\text{counter})}] \times [P_{O_2(\text{counter})}/P_{O_2(\text{working})}]^{1/2}. \quad (6)$$

Table 1
OCV responses of the electrochemical cell with the mixtures of 0–1600 ppm NO, 0–8400 ppm H_2, and 5% O_2 in Ar at 250 °C

NO (ppm)	H_2 (ppm)	OCV (mV)
200	0	50.6
800	0	53.5
1600	0	55.2
0	2800	−141
0	5600	−169
0	8400	−185

This means that $Sn_{0.9}In_{0.1}P_2O_7$ exhibits proton conduction rather than oxide ion conduction under the present conditions. In contrast, when a small amount of H_2 coexisted with excess O_2, the OCV was shifted significantly toward the negative direction, with the value dependent on the H_2 concentration; for example, the OCV reached −185 mV at 8400 ppm. It is important to note here that, assuming that all of the 8400-ppm H_2 is converted to H_2O over the Pt/C working electrode, the O_2 concentration will change from 5% to 4.58%, and the H_2O vapor concentration will increase from 0.6% to 1.44%. According to Nernst's equation (6), the OCV will change from +20 to −0.6 mV. The large discrepancy between the measured and theoretical OCV values implies that the behavior observed for the Pt/C working electrode is non-Nernstian [21], suggesting that the reaction rate of reaction (3) is much higher than that of the O_2 reduction and H_2O vapor oxidation. In contrast, when a small amount of NO was present in an excess of O_2, the electrochemical cell showed moderately positive OCVs, indicating that reaction (4) proceeded at a faster rate. Preliminary experiments showed that about 9% of the supplied NO was converted into NO_2 through catalytic oxidation over the Pt/C working electrode. It appears that the following reaction also contributes to the observed OCV to some extent:

$$NO_2 + 4H^+ + 4e^- \rightarrow \frac{1}{2}N_2 + 2H_2O. \quad (7)$$

Based on the above results, if the Pt/C working electrode were supplied with a mixture of NO, H_2, and O_2, then a galvanic cell would be formed at the electrode–electrolyte interface. Because the electrode also functions as a lead wire, the galvanic cell would then be short-circuited. As a result, both reactions (3) and (4) proceed simultaneously at the Pt/C working electrode, as displayed in Scheme 1. We next provide experimental evidence for this scheme.

We measured the transient change in the NO_x concentration in the outlet gas from the Pt/C working electrode under open-circuit conditions at 250 °C, with the NO and O_2 concentrations maintained at 800 ppm and 5%, respectively. As shown in Fig. 2, the reduction of NO_x did not occur in the absence of H_2. This is due to inhibition of this reaction by oxygen adsorbed over the Pt surface from the gas phase [22]. As the H_2 concentration increased in the gas mixture, the NO_x concentration decreased and N_2 concentration increased. In this case, the N_2 selectivity was as high as ∼84% for all H_2 concentrations evaluated. We discuss the high N_2 selectivity later. Another important result is that NO_x was not reduced over a Pt-free carbon electrode, indicating that the Pt catalyst plays an important role in H_2 SCR. In other words, $Sn_{0.9}In_{0.1}P_2O_7$ itself has no catalytic activity for H_2 SCR.

We studied the catalytic activity of the Pt/C working electrode for H_2 SCR using various solid electrolytes at 250 °C.

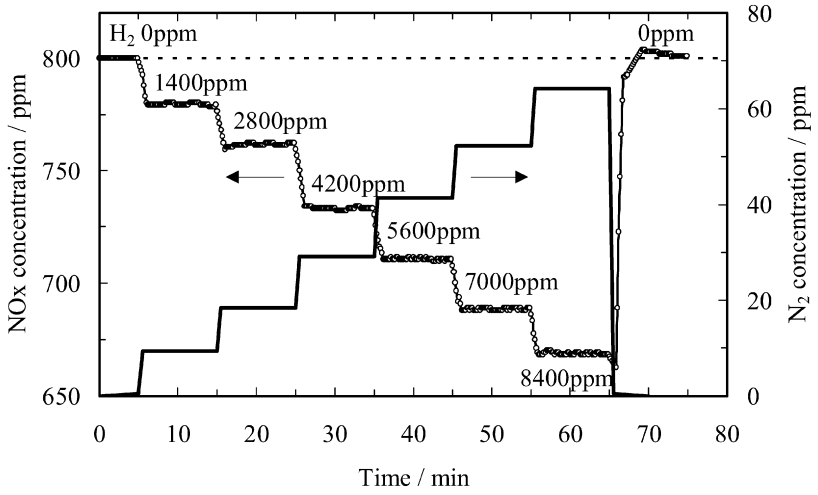

Fig. 2. Transient changes in NO and N_2 concentrations in the outlet gas from the Pt working electrode at 250 °C. The reactant gas was 800 ppm NO, 0–8400 ppm H_2, and 5% O_2 in Ar at a flow rate of 50 mL min^{-1}.

Plots of the NO_x conversion as a function of H_2 concentration are shown in Fig. 3. Comparing the results for $Sn_{0.9}In_{0.1}P_2O_7$ with those for silica and YSZ (Fig. 3a) shows that using $Sn_{0.9}In_{0.1}P_2O_7$ significantly enhanced NO_x conversion. Note that under the present conditions, $Sn_{0.9}In_{0.1}P_2O_7$ shows a proton conductivity of 0.2 S cm^{-1}, whereas the other two electrolytes show extremely low ion conductivities (10^{-6}–10^{-4} S cm^{-1}). This result supports the validity of Scheme 1. In contrast, our previous study demonstrated that the proton conductivity of $Sn_{1-x}In_xP_2O_7$ ($x = 0$–0.1) increased with increasing amounts of In^{3+} dopants and H_2O vapor concentration in the atmosphere [17]. In both cases (Figs. 3b and 3c), the increased proton conductivity enhanced NO_x conversion. This result can be explained by assuming that one or more of the three steps shown in Scheme 1 (H_2 oxidation, proton migration, and NO reduction) is promoted by increasing the proton conductivity of $Sn_{1-x}In_xP_2O_7$. It is also suggested that H_2O vapor coexisting in the exhaust imparts a positive effect on H_2 SCR, which is very useful under actual conditions that include % level of H_2O vapor.

We also studied the catalytic activity of the Pt/C working electrode for H_2 SCR under different operating conditions. Fig. 4a shows that NO_x conversion was strongly influenced by O_2 concentration. The Pt/C working electrode became less active as the O_2 concentration increased. GC measurement of the outlet gas from the Pt/C working electrode showed that the H_2 concentration decreased from 8400 to 3200 ppm with increasing O_2 concentration from 2% to 9%. We hypothesize that this is due to the catalytic combustion of H_2 decreasing the NO_x conversion. Another possible reason is that the following reaction could be enhanced by increasing the O_2 concentration:

$$O_2 + 4H^+ + 4e^- \rightarrow 2H_2O. \quad (8)$$

Because reaction (8) competes with reaction (4) in reacting with protons at the electrolyte–electrode interface, NO_x conversion can be considered decreased due to an increase in O_2 concentration. A similar competition has been reported for NO_x electrolyzers using proton and oxide-ion conductors [23]. As can be seen from Fig. 4b, NO_x conversion also was strongly influenced by temperature. High-temperature operation was unfavorable for the present H_2 SCR. Also, in this case, a decrease in H_2 concentration at increasing temperature, causing decreased NO_x conversion, was confirmed for the outlet gas from the Pt/C working electrode. However, the fact that reaction (8) was catalyzed at increasing temperature, which also can decrease NO_x conversion, cannot be neglected. It is well known that the cathodic reaction corresponding to reaction (8) is promoted by an increase in temperature in polymer electrolyte fuel cells (PEFCs) [24]. On the other hand, NO_x conversion was shown to be independent of CO_2 concentration (see Fig. 4c). This is strong evidence that CO_2 functions as an inert gas for both H_2 combustion and reactions (3), (4), and (8).

If the reaction mechanism for the present H_2 SCR is based on Scheme 1, then it can be assumed that reactions (3) and (4) proceed simultaneously at the Pt/C working electrode. These reaction rates are equal due to the formation of a local cell and its subsequent self-discharge, resulting in the appearance of a mixed potential [25–27]. To clarify this mechanism, we measured the anodic polarization curve of 8400 ppm H_2 diluted with Ar and the cathodic polarization curve of a mixture of 800 ppm NO and 5% O_2 in Ar at 250 °C. The results summarized in Fig. 5, show that the direction of the cathodic current was reversed. The intersection point of the anodic and cathodic polarization curves, which corresponds to the mixed potential [25–27], was found to be at −203 mV. This mixed potential was somewhat more negative than the OCV value of −177 mV found when a mixture of 800 ppm NO, 8400 ppm H_2, and 5% O_2 in Ar was supplied to the Pt/C working electrode at 250 °C. One possible explanation for this discrepancy is that whereas all of the 8400-ppm H_2 could participate in the anodic reaction in the polarization measurement, a part of the H_2 was burned in the OCV measurement. Therefore, to eliminate any effect due to the lost H_2, the above two measurements were made in the absence of O_2. As shown in Fig. 5, the mixed potential was at −680 mV, almost in agreement with the observed OCV value of −689 mV. This near agreement demonstrates

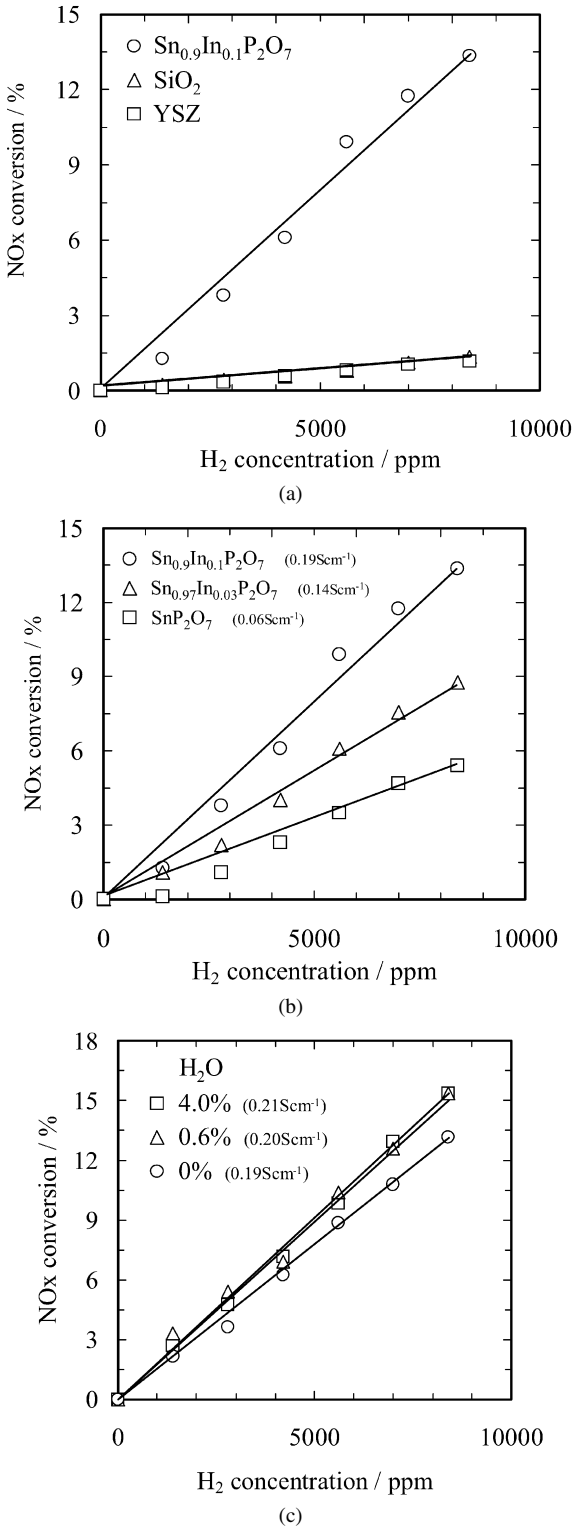

Fig. 3. Plots of NO_x conversion as a function of H_2 concentration (a) using $Sn_{0.9}In_{0.1}P_2O_7$, silica glass and YSZ as electrolyte substrates, (b) using $Sn_{1-x}In_xP_2O_7$ ($x = 0$–0.1) as electrolyte substrates, and (c) at H_2O-vapor concentrations of 0–4%. The operating temperature was maintained at 250 °C. The reactant gas was 800 ppm NO, 0–8400 ppm H_2, and 5% O_2 in Ar at a flow rate of 50 mL min^{-1}.

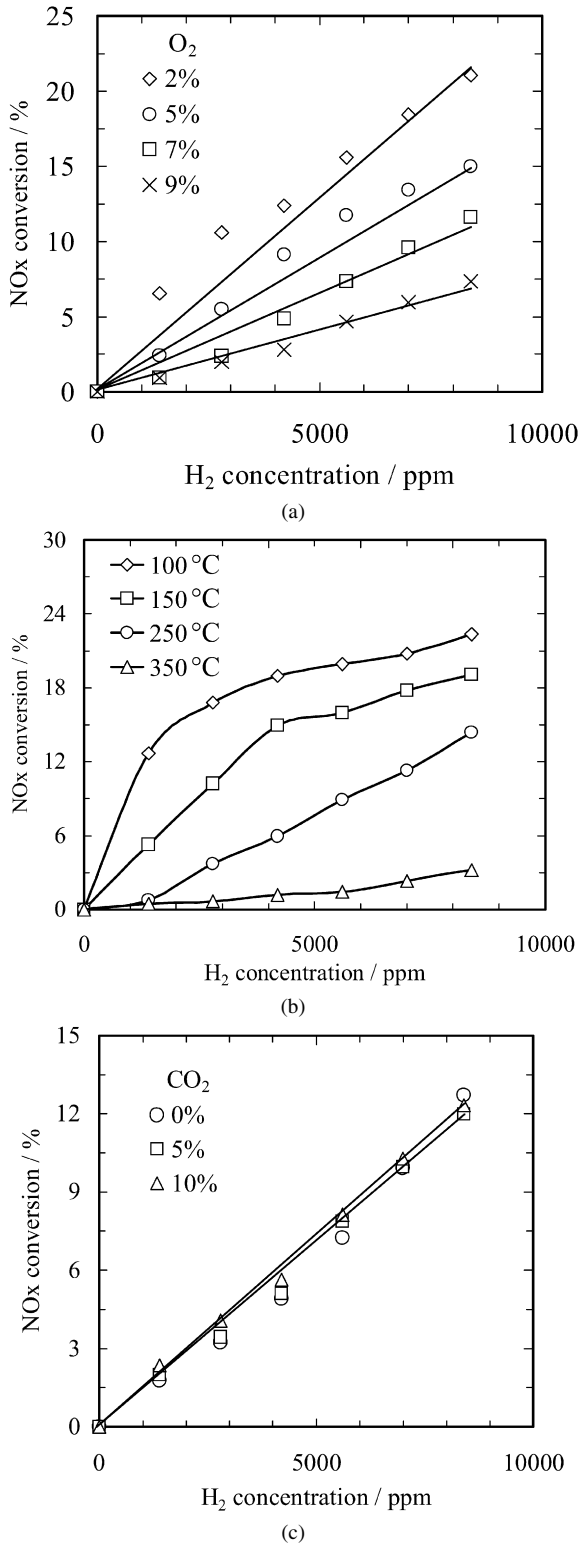

Fig. 4. Plots of NO_x conversion as a function of H_2 concentration (a) at O_2 concentrations of 2–9%, a CO_2 concentration of 0% and at 250 °C, (b) at temperatures of 100–350 °C and at an O_2 concentration of 5% and a CO_2 concentration of 0%, and (c) at a CO_2 concentration of 0–10% and an O_2 concentration of 5% at 250 °C. The reactant gas was 800 ppm NO, 0–8400 ppm H_2, 2–9% O_2, 0–10% CO_2 in Ar at a flow rate of 50 mL min^{-1}.

that reactions (3) and (4) actually occur at the Pt/C working electrode. More importantly, the short-circuit current shown in Fig. 5 reached 50 mA in the presence of O_2 and 12 mA in the absence of O_2, higher than the theoretical current of 3 mA calculated from Faraday's law when all of the 800-ppm NO was electrochemically reduced to N_2 according to reaction (4). This

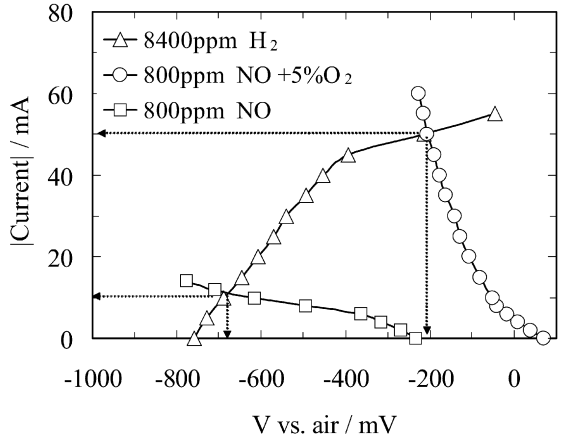

Fig. 5. Anodic polarization curve for 8400 ppm H_2 in Ar and cathodic polarization curves for a mixture of 800 ppm NO and 5% O_2 in Ar and 800 ppm NO in Ar at the Pt/C working electrode at 250 °C. The direction of the cathodic current is reversed.

result implies that the short-circuit current was sufficiently high to explain the NO_x conversions shown in Figs. 3 and 4, thus making Scheme 1 more reliable.

Here it is interesting to compare the NO_x reduction based on the mixed potential in the present study with the NO_x reduction in the electrolyzer reported previously [19]. For instance, the NO_x conversion reached 6% at a H_2 concentration of 4200 ppm, as shown in Fig. 3. On the other hand, equivalent hydrogen species production would be expected at the cathode on application of a current density of 30 mA to the electrochemical cell. The previous study showed a NO_x conversion of 9% at 30 mA, higher than the above conversion. The difference can be explained by the more significant catalytic combustion of H_2 in the present method compared with the previous method.

3.2. $Pt/Sn_{0.9}In_{0.1}P_2O_7$ catalyst

To clarify whether Scheme 1 is applicable to the $Pt/Sn_{0.9}In_{0.1}P_2O_7$ catalyst, catalyst performance was tested at 50–350 °C. Fig. 6 shows the NO_x conversion over the $Pt/Sn_{0.9}In_{0.1}P_2O_7$ catalyst as a function of temperature, with the data observed for the electrochemical cell with the Pt/C working electrode included for comparison. For all Pt values, the catalyst showed relatively high NO_x conversion between 50 and 350 °C, with NO_x conversion reaching a maximum at about 100 °C. These temperature profiles are qualitatively similar to those observed for the electrochemical cell. Another similarity between the catalyst and electrochemical cell, in N_2 selectivity, was confirmed. As shown in Fig. 7, both the catalyst and electrochemical cell showed N_2 selectivity values of >80% over the whole temperature range. These similarities suggest that H_2 SCR proceeded in a similar manner over the catalysts and the electrochemical cell. On the other hand, Fig. 6 also showed that higher NO_x conversions over the catalysts than over the electrochemical cell at all temperatures tested, with this tendency growing with increasing Pt content. This finding can be explained by the fact that the $Pt/Sn_{0.9}In_{0.1}P_2O_7$ interface assigned to an electrochemical reaction site is more highly dispersed for

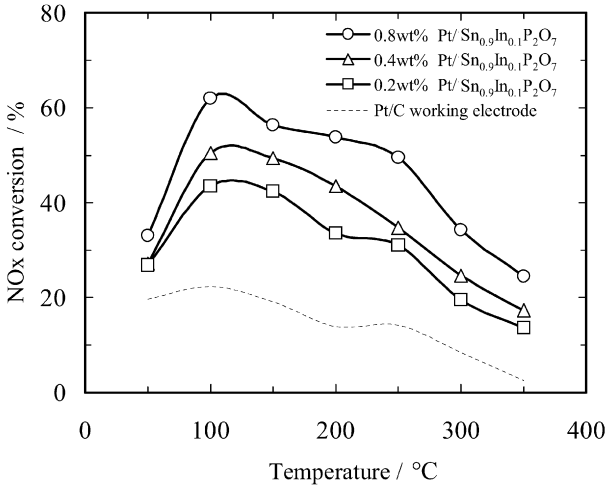

Fig. 6. Plots of NO_x conversion as a function of temperature over the $Pt/Sn_{0.9}In_{0.1}P_2O_7$ catalyst (Pt content = 0.2–0.8 wt%) and the Pt/C working electrode. The reactant gas was 800 ppm NO, 8400 ppm H_2, and 5% O_2 in Ar at a flow rate of 50 mL min^{-1}.

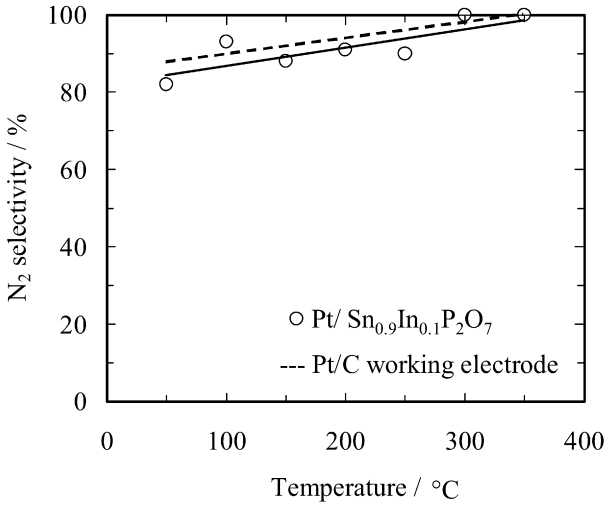

Fig. 7. Plots of N_2 selectivity as a function of temperature over the $Pt/Sn_{0.9}In_{0.1}P_2O_7$ catalyst (Pt content = 0.8 wt%) and the Pt/C working electrode. The reactant gas was 800 ppm NO, 8400 ppm H_2, and 5% O_2 in Ar at a flow rate of 50 mL min^{-1}.

the catalyst than for the electrochemical cell, because the working electrode was merely placed on the electrolyte surface.

As described above, the $Pt/Sn_{0.9}In_{0.1}P_2O_7$ catalyst was characterized by a wide operating temperature window and remarkable N_2 selectivity. It can be speculated that these characteristics can be ascribed to the electrochemical activation of both H_2 and NO resulting from reactions (3) and (4), respectively. This suggests that the catalyst performance would be further improved by promoting reactions (3) and (4). Fig. 5 shows that the polarization resistance of 30 Ω cm^2 for reaction (4) is much higher than the resistance of 12 Ω cm^2 for reaction (3), indicating that reaction (4) rather than reaction (3) should be promoted. Toward this end, we first evaluated various working electrodes using the electrochemical cell. Fig. 8 shows the plots of NO_x conversion as a function of the H_2 concentration at 250 °C. Only the PtRh/C working electrode showed higher

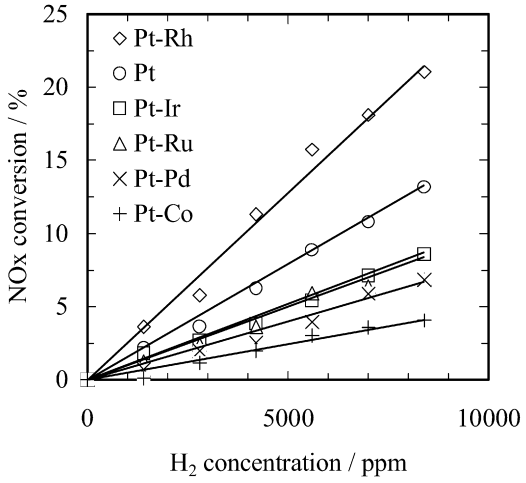

Fig. 8. Plots of NO_x conversion as a function of H_2 concentration over the PtM/C working electrodes (M = Rh, Ir, Ru, Pd, Co) at 250 °C. The reactant gas was 800 ppm NO, 0–8400 ppm H_2, and 5% O_2 in Ar at a flow rate of 50 mL min^{-1}.

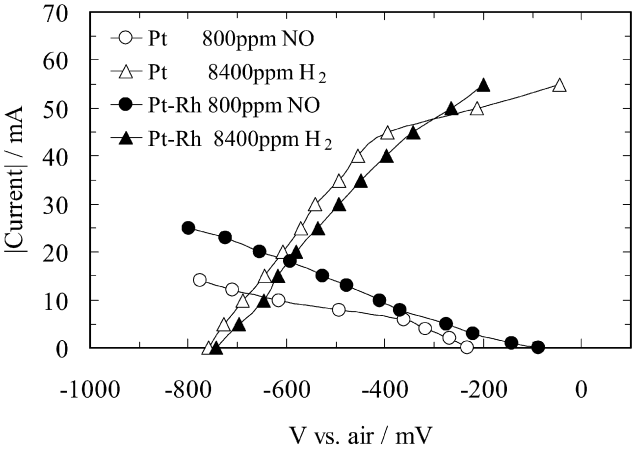

Fig. 9. Anodic polarization curves for 8400 ppm H_2 in Ar and cathodic polarization curves for 800 ppm NO in Ar at the PtRh/C and Pt/C working electrodes at 250 °C. The direction of the cathodic current is reversed.

catalytic activity for H_2 SCR than the Pt/C working electrode; NO_x conversion was about 1.5 times greater at the PtRh/C working electrode than at the Pt/C working electrode at all tested H_2 concentrations. The impedance spectra of the electrochemical cells obtained with these working electrodes further clarify this point; the order of electrode-reaction resistance was PtRh (3.0 Ω) < Pt (3.7 Ω) < PtRu (4.1 Ω) < PtPd (6.6 Ω) < PtIr (6.8 Ω) < PtCo (7.4 Ω), which is roughly in agreement with the order of the NO_x conversion shown in Fig. 8. This result suggests that adding Rh to Pt activates one or both of reactions (3) and (4), whereas adding other metals to Pt deactivates these reactions.

To better understand the beneficial effect of Rh on the catalytic activity for H_2 SCR, we measured the anodic polarization curve of 8400-ppm H_2 diluted with Ar and the cathodic polarization curve of 800-ppm NO diluted with Ar at 250 °C. Fig. 9 shows the comparative results observed for the PtRh/C and Pt/C working electrodes. There was little difference in the anodic polarization curve corresponding to reaction (3) between the

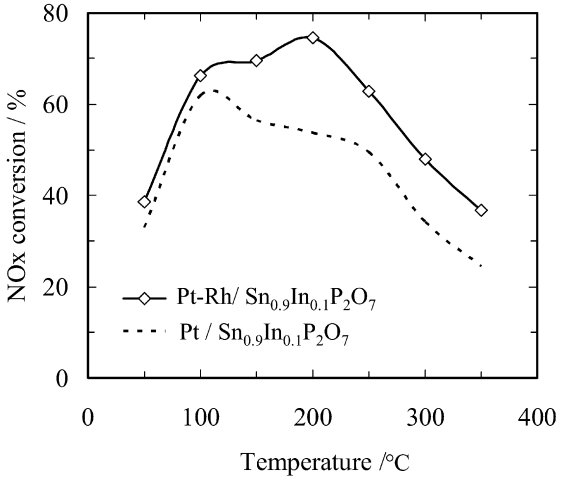

Fig. 10. Plots of NO_x conversion as a function of temperature over PtRh/$Sn_{0.9}In_{0.1}P_2O_7$ (PtRh content = 0.8 wt%, Pt/Rh atomic ratio = 4) and Pt/$Sn_{0.9}In_{0.1}P_2O_7$ (Pt content = 0.8 wt%) catalysts. The reactant gas was 800 ppm NO, 8400 ppm H_2, and 5% O_2 in Ar at a flow rate of 50 mL min^{-1}.

two working electrodes, indicating that Rh does not contribute to H_2 oxidation at the electrode–electrolyte interface. To the best of our knowledge, no previous study has shown that Rh is a useful catalyst for the anodic reaction of H_2 in PEFCs. On the other hand, the difference between the two working electrodes was more pronounced for the cathodic polarization curve corresponding to reaction (4). Clearly, the addition of Rh to Pt enhanced the catalytic activity for NO_x reduction. This result is consistent with results from our previous study in which the PtRh/C working electrode showed higher sensitivities in the mixed-potential-type NO_x sensor compared with the Pt/C working electrode [28].

Pt and Rh were supported on $Sn_{0.9}In_{0.1}P_2O_7$, and the catalyst performance for H_2 SCR was measured. As in the case of the electrochemical cell, the PtRh/$Sn_{0.9}In_{0.1}P_2O_7$ catalyst exhibited a beneficial effect of Rh on catalytic activity, as shown in Fig. 10. One obvious finding shown in this figure is that the effect was greater at higher temperatures; for example, NO_x conversion reached about 40% at 350 °C. Another obvious feature is that two conversion maxima were observed at 100 and 200 °C. This is a well-known behavior for various SCR catalysts reported thus far; the low-temperature peak is assigned to the direct reduction of NO, whereas the high-temperature peak is assigned to the reduction of NO_2 generated in situ [29,30]. Considering these results, the addition of Rh to the catalyst can be proposed to catalyze reaction (7) as well as reaction (4). In contrast, Fig. 11 shows higher N_2 selectivity values for PtRh/$Sn_{0.9}In_{0.1}P_2O_7$ than for Pt/$Sn_{0.9}In_{0.1}P_2O_7$ at 50–350 °C. In particular, it is noteworthy that a N_2 selectivity of 89% was achieved at 50 °C. As described earlier, N_2 formation is due to the reaction of two $N_{(ad)}$ atoms with one another [11]. Therefore, we suggest that $N_{(ad)}$ formation is increased by the promotion of reactions (4) and (7), improving N_2 selectivity.

Based on the results described above, it can be concluded that proton conduction in $Sn_{0.9}In_{0.1}P_2O_7$ is a contributing factor to the high NO_x conversion and N_2 selectivity over a wide temperature range. This can be well understood by consider-

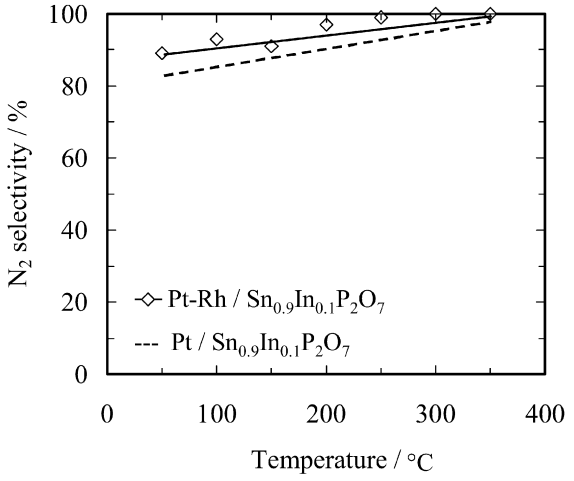

Fig. 11. Plots of N_2 selectivity as a function of temperature over PtRh/$Sn_{0.9}In_{0.1}P_2O_7$ (PtRh content = 0.8 wt%, Pt/Rh atomic ratio = 4) and Pt/$Sn_{0.9}In_{0.1}P_2O_7$ (Pt content = 0.8 wt%) catalysts. The reactant gas was 800 ppm NO, 8400 ppm H_2, and 5% O_2 in Ar at a flow rate of 50 mL min^{-1}.

ing Scheme 1. Still other factors may play an important role in H_2 SCR; for example, it has been proposed that NO can be adsorbed on oxide ion vacancies formed in oxide supports, promoting NO dissociation [15]. $Sn_{0.9}In_{0.1}P_2O_7$ may have oxide ion vacancies due to the substitution of In^{3+} for some of the Sn^{4+}; however, as described earlier, the proton transport number of ca. 1 indicates that protons serve almost entirely as positive point defects in $Sn_{0.9}In_{0.1}P_2O_7$. This defect structure suggests that the above effect is very small. NH_3 formation through NO reduction by H_2, followed by reaction with NO, also has been proposed [12]. In this case, some acidic catalyst supports can effectively store NH_3 as NH_4^+, resulting in high H_2 SCR activity [13]. Although $Sn_{0.9}In_{0.1}P_2O_7$ is also a solid acid, it showed distinct catalytic activity related to the proton conductivity, which cannot be explained by the above effect. In addition, the specific surface area of $Sn_{0.9}In_{0.1}P_2O_7$ was <0.5 m^2 g^{-1}, which may be too small to allow significant adsorption of NH_3.

4. Conclusion

The present study has proposed a new scheme for H_2 SCR based on proton conduction in $Sn_{0.9}In_{0.1}P_2O_7$, which was used as a catalyst support. In a mixture of NO, H_2, and O_2 in Ar, H_2 dissociated to protons and electrons at an anodic site of the Pt/C working electrode, causing a negative potential. In contrast, NO_x reacted with protons and electrons to form N_2 and H_2O at a cathodic site of the Pt/C working electrode, resulting in a positive potential. As a result, an electrochemical local cell was formed at the Pt/C working electrode, followed by self-discharge. This scheme also could be realized in the H_2 SCR for Pt/$Sn_{0.9}In_{0.1}P_2O_7$. Two major catalytic properties were observed: catalytic activity over a wide temperature range (50–350 °C) and remarkably high N_2 selectivity (>80%). A further improvement in catalytic performance was achieved by adding Rh to Pt. NO_x conversion was a maximum 1.4 times greater than those observed for Pt/$Sn_{0.9}In_{0.1}P_2O_7$; N_2 selectivity was >89% at all temperatures tested. Our findings demonstrate that the beneficial effect of Rh is based on promotion of the cathodic reaction of NO.

References

[1] L.R. Raber, Chem. Eng. News 75 (1997) 10.
[2] H. Bosch, F. Janssen, Catal. Today 2 (1988) 369.
[3] G. Busca, L. Lietti, G. Ramis, F. Berti, Appl. Catal. B 18 (1998) 1.
[4] P. Forzatti, Appl. Catal. A 222 (2001) 221.
[5] R.M. Heck, Catal. Today 53 (1999) 519.
[6] J.-H. Lee, H.H. Kung, Catal. Lett. 51 (1998) 1.
[7] M. Konsolakis, N. Macleod, J. Issac, I.V. Yentekakis, R.M. Lambert, J. Catal. 193 (2000) 330.
[8] P. Denton, A. Giroir-Fendler, H. Praliaud, M. Primet, J. Catal. 189 (2000) 410.
[9] E. Shustorovich, A.T. Bell, Surf. Sci. 289 (1993) 127.
[10] R. Burch, T.C. Watling, Catal. Lett. 37 (1996) 51.
[11] R. Burch, M.D. Coleman, Appl. Catal. B 23 (1999) 115.
[12] T. Nanba, C. Kohno, S. Masukawa, J. Uchisawa, N. Nakayama, A. Obuchi, Appl. Catal. B 46 (2003) 353.
[13] J. Shibata, M. Hashimoto, K.-i. Shimizu, H. Yoshida, T. Hattori, A. Satsuma, J. Phys. Chem. B 108 (2004) 18327.
[14] K. Yokota, M. Fukui, T. Tanaka, Appl. Surf. Catal. 121/122 (1997) 273.
[15] C.N. Costa, V.N. Stathopoulos, V.C. Belessi, A.M. Efstathiou, J. Catal. 197 (2001) 350.
[16] M. Nagao, A. Takeuchi, P. Heo, T. Hibino, M. Sano, A. Tomita, Electrochem. Solid-State Lett. 9 (2006) A105.
[17] M. Nagao, T. Kamiya, P. Heo, A. Tomita, T. Hibino, M. Sano, J. Electrochem. Soc. 153 (2006) A1604.
[18] P. Heo, H. Shibata, M. Nagao, T. Hibino, M. Sano, J. Electrochem. Soc. 153 (2006) A897.
[19] M. Nagao, T. Yoshii, T. Hibino, M. Sano, A. Tomita, Electrochem. Solid-State Lett. 9 (2006) J1.
[20] H. Uchida, N. Maeda, H. Iwahara, J. Appl. Electrochem. 12 (1982) 645.
[21] W.J. Fleming, J. Electrochem. Soc. 124 (1977) 21.
[22] A. Amirnazmi, M. Boudart, J. Catal. 39 (1975) 383.
[23] K. Kammer, Appl. Catal. B 58 (2005) 33.
[24] B.C.H. Steel, A. Heinzel, Nature 414 (2001) 345.
[25] N. Miura, G. Lu, N. Yamazoe, H. Kurosawa, M. Hasei, J. Electrochem. Soc. 143 (1996) L33.
[26] R. Balasubramaniam, Scripta Mater. 34 (1996) 127.
[27] R. Mukundan, E.L. Brosha, D.R. Brown, F.H. Garzon, Electrochem. Solid-State Lett. 2 (1999) 412.
[28] M. Nagao, Y. Namekata, T. Hibino, M. Sano, A. Tomita, Electrochem. Solid-State Lett. 9 (2006) H48.
[29] A. Ueda, T. Nakao, M. Azuma, T. Kobayashi, Catal. Today 45 (1998) 135.
[30] N. Macleod, R.M. Lambert, Appl. Catal. B 35 (2002) 269.